Ovariectomy modifies lipid metabolism of retroperitoneal white fat in rats: a proteomic approach

Valter T. Boldarine[1], Amanda P. Pedroso[1], Caroline Brandão-Teles[2], Edson G. LoTurco[6], Cláudia M.O. Nascimento[1], Lila M. Oyama[1], Allain A. Bueno[7], Daniel Martins-de-Souza[2,3,4,5], Eliane B. Ribeiro[1]

[1]Universidade Federal de São Paulo, Escola Paulista de Medicina, Departamento de Fisiologia, São Paulo, SP, Brazil.

[2]Laboratory of Neuroproteomics, Department of Biochemistry and Tissue Biology, Institute of Biology, University of Campinas (UNICAMP), Campinas, Brazil.

[3]Instituto Nacional de Biomarcadores em Neuropsiquiatria (INBION) Conselho Nacional de Desenvolvimento Científico e Tecnológico, São Paulo, Brazil.

[4]Experimental Medicine Research Cluster (EMRC), University of Campinas, Campinas 13083-862, SP, Brazil.

[5]D'Or Institute for Research and Education (IDOR), São Paulo, Brazil.

[6]Universidade Federal de São Paulo, Escola Paulista de Medicina, Departamento de Cirurgia, Divisão de Urologia e Reprodução Humana, São Paulo, Brazil.

[7]Department of Biological Sciences, College of Health, Life and Environmental Sciences, University of Worcester, Worcester, United Kingdom

Corresponding author:

Valter Tadeu Boldarine
Universidade Federal de São Paulo, Departamento de Fisiologia
Rua Botucatu 862, 2º andar
Vila Clementino, 04023-062, São Paulo, SP, Brasil
E-mail: valtertadeuboldarine@gmail.com
Phone/Fax: 55 11 5576-4765

Abstract: Menopause is often accompanied by visceral obesity. With the aim of exploring the consequences of ovarian failure on visceral fat, we evaluated the effects of ovariectomy and estrogen replacement on the proteome/phosphoproteome and on the fatty acids profile of the retroperitoneal adipose depot (RAT) of rats. Eighteen three months old female Wistar rats were either ovariectomized or sham-operated and fed with standard chow for three months. A sub-group of ovariectomized rats received estradiol replacement. RAT samples were analyzed using data-independent acquisitions LC-MS/MS and pathway analysis was performed with the differentially expressed/phosphorylated proteins. RAT lipid profile was analyzed by gas chromatography.

Ovariectomy induced high adiposity and insulin resistance and promoted alterations in protein expression and phosphorylation. Pathway analysis showed that 5 pathways were significantly affected by ovariectomy, namely metabolism of lipids (included fatty acid metabolism and mitochondrial fatty acid β-oxidation), fatty acyl-CoA biosynthesis, innate immune system (included neutrophil degranulation), metabolism of vitamins and cofactors, and integration of energy metabolism (included ChREBP activates metabolic gene expression). Lipid profile analysis showed increased palmitic and palmitoleic acids content. The analysis of the data indicated that ovariectomy favored lipogenesis while it impaired fatty acids oxidation, and induced a pro-inflammatory state in the visceral adipose tissue. These effects are consistent with the findings of high adiposity, hyperleptinemia, and impaired insulin sensitivity. The observed alterations were partially attenuated by estradiol replacement. The data point to a role of disrupted lipid metabolism in adipose tissue in the genesis of obesity after menopause.

Keywords – menopause; retroperitoneal adipose tissue; proteome/phosphoproteome; lipid profile; estrogen replacement.

1. Introduction

The cessation of ovarian hormones production in menopause is often followed by increased body weight gain and adiposity, associated with obesity-related co-morbidities (11, 28). In both humans and rodents, a role of estrogens in metabolic, immune, and inflammatory processes has been established, although the complexity by which these effects occur is not fully understood (20, 45). The lack of estrogens after menopause has been associated with a shift of fat distribution from subcutaneous to visceral, with impairment of the sensitivity to insulin and leptin, predisposition to diabetes and to anxiety and depressive disorders (5, 14, 23).

In both humans and rats, the visceral (or abdominal) adipose tissue comprises mesenteric, retroperitoneal, perirenal, and gonadal depots. Additionally, humans have the omental depot (38). A depot-specificity of functions has been described for the adipose tissue, which may result from differences intrinsic to pre-adipocytes and to factors secreted by neighboring organs (62). During the development of obesity, the visceral adipose tissue suffers a higher degree of hypertrophy and macrophage infiltration than the subcutaneous depots, leading to a high production of inflammatory mediators that contribute substantially to the pathophysiology of obesity complications (40, 46).

Several disruptions of the metabolism of visceral adipose tissue have been reported in ovariectomized rodent models. Increased conversion of cortisone to cortisol, due to increased expression of type 1 11β-hydroxysteroid dehydrogenase, has been found in visceral but not in subcutaneous adipose depots, contributing to fat redistribution (3). Decreased glutathione peroxidase activity and superoxide dismutase protein levels, indicating impairment of anti-oxidant status, as well as low mRNA levels of the anti-inflammatory hormone adiponectin, have also been observed (1).

Using a two-dimensional gel electrophoresis-based proteomic approach, a recent study described that ovariectomy affected proteins involved in intermediate metabolism, energy transduction, cell structure, and immune system, in the periovarian adipose tissue of rats (2). The use of a more sensitive and accurate proteomic technique could help unravel a more expressive number of proteins and pathways affected by ovarian failure in the visceral fat.

Moreover, the identification of changes in protein phosphorylation is of high relevance, as it plays a pivotal role in a multitude of cellular functions.

Additionally, perturbations of visceral adipose tissue functions have been associated with its fatty acids composition in several conditions, such as diet-induced obesity and diabetes (6, 63). However, data on the effects of obesity induced by the loss of ovarian hormones in visceral adipose tissue fatty acid composition are scarce. One study reported increased levels of short-chain saturated fatty acids levels in the visceral fat of postmenopausal women (67). Further studies on the subject are necessary.

Aiming at expanding our knowledge on the consequences of ovarian failure on visceral fat, the present study examined the effects of ovariectomy and of estrogen replacement on the proteome/phosphoproteome as well as on the fatty acid profile of the retroperitoneal fat of rats.

2. Materials and Methods

2.1 Experimental procedures

The experiments were performed in accordance with the Committee in Research Ethics of the Universidade Federal de São Paulo (CEUA nº: 2172030315/ 2016), which follow the guidelines of the Conselho Nacional de Controle de Experimentação Animal (CONCEA). The present data is part of our previously published investigation in which we evaluated the effects of ovariectomy, aligned or not to high-fat diet feeding, on metabolic and behavior parameters of rats (5). Briefly, the female *Wistar* rats (twelve-week-old) were either ovariectomized (Ovx group, n=12) or sham operated (Sham group, n=6) under ketamine/xylazine anesthesia (66/33mg/kg, ip). A sub-set of Ovx animals received 17β-estradiol replacement (Ovx+E2 group), via subcutaneous pellets (0.25 mg/pellet, 90-day release; Innovative Research of America, Sarasota, Florida, USA). The daily dose of estrogen released was 2.8 μg/day/90 days, yielding a daily dose range of 0.010 to 0.008 mg/Kg/day, considering the mean initial and final body weights during the 12 weeks of treatment. One dose of penicillin (60.000U. i.m.) and ibuprofen (1 mg/kg body weight, v.o.) was given to all animals after the surgery. Additionally,

111 they received one ibuprofen dose per day for the 2 subsequent days. They were maintained
112 under a 12h light/dark cycle (lights on at 6 am) and 23 ± 1°C temperature with food (2.87
113 kcal/g, 15% of energy from fat, Nuvilab CR-1, Nuvital Nutrientes SA, Colombo, PR, Brazil)
114 and water ad libitum for 12 weeks. Body weight and 24-h food mass intake were measured
115 once a week. Feed efficiency was calculated as: (body weight gain / energy intake) x 100.
116 Euthanasia was conducted under thiopental anesthesia (80mg/kg, ip) after a 24-h fasting.
117 Trunk blood was collected and white fat pads (retroperitoneal, gonadal and mesenteric) were
118 dissected, weighed, and frozen in liquid nitrogen. All tissue and serum samples were stored at -
119 80ºC. The uteri were weighed for confirmation of completeness of ovaries removal.
120
121 *2.2 Serum and tissue cytokines measurements*
122
123 Serum measurements and HOMA index were conducted as previously described (5).
124 RAT content of TNF-α (sensitivity – 2.4 ng/mL; intra-assay precision- 4.98%; inter-assay
125 precision- 9.44%) and IL-6 (sensitivity – 0.7 ng/mL; intra-assay precision- 3.96%; inter-assay
126 precision- 8.64%) were also determined by Elisa (R&D Systems, Minneapolis, MN, USA).
127
128 *2.3 Retroperitoneal fat proteome and phosphoproteome analyses*
129
130 Aliquots (800 mg) of RAT fat pads were homogenized in 1mL of buffer containing 50
131 mM ammonium bicarbonate, 1% sodium deoxycholate (m/v), and deionized water (51), with
132 the addition of a protease/phosphatase inhibitor cocktail (Thermo Scientific, Rockford, IL,
133 USA), and centrifuged at 19,000 x g for 30 minutes at 4^{o}C. Protein concentration in the
134 supernatants was determined using a Pierce BCA assay (Thermo Scientific, Rockford, IL,
135 USA). Aliquots of 200 µg of protein were diluted in 50 mM ammonium bicarbonate to a final
136 volume of 85 µL. Samples were then subjected to reduction with 2.5 µL of 100 mM DTT at
137 60^{o}C for 30 min and alkylation with 2.5 µL of 300 mM iodoacetamide, at room temperature for
138 30 min. Proteins were digested overnight using trypsin (Promega, Fitchburg, WI, USA) at a
139 1:100 (wt:wt) enzyme:protein ratio at 37^{o}C. After digestion, samples were centrifuged at

19,000 x g for 15 minutes at 4ºC, the supernatants were collected and an equal volume of ethyl acetate was added (36). Then, trifluoroacetic acid was added to a final concentration of 0.5%. Samples were homogenized in vortex and centrifuged at 19,000 x g for 5 minutes at 4°C. Supernatants were collected, transferred to Millex-GV filters (Millipore, Burlington, MA, USA), recovered, dried in a vacuum concentrator centrifuge (Eppendorf, Hamburg, HH, Germany), and stored at -80°C until mass spectrometry analysis.

2.4 Liquid-chromatography mass spectrometry

After reconstitution of the samples in 1 % (v/v) formic acid, protein content was determined fluorimetricaly (Qubit® 3.0 Fluorometer, Thermo Scientific, Rockford, IL, USA) and the final concentration was adjusted to 0.5 µg/µL. The proteomic and phosphoproteomic analyses were performed by data-independent acquisitions liquid-chromatography mass spectrometry (ACQUITY UPLC M-Class coupled to Synapt G2-Si mass spectrometer) (Waters, Milford, MA, USA). An ACQUITY UPLC HSS T3 nanoACQUITY Column (100 Å. 1.8 µm. 75 µm × 150 mm., Waters) was used for peptides separation (1µg) in acetonitrile gradient from 7% (v/v) for 54 min, and then increased to 80% of acetonitrile for 13 min, at a flow rate of 500 nL/min). Data were acquired using nanoESI ionization on positive mode, in $HDMS^E$ mode using Transfer MS Collision Energy Low (eV) 19.0 and Transfer MS Collision Energy High (eV) 53.0. Human Glu-fibrinopeptide B was used for mass spectrometer calibration. MS identification was made between 50 and 2000 *m/z*.

2.5 Database search

Mass spectrometry data processing and database search against Rattus norvegicus sequences (UniProtKB/Swiss-Prot database, www.uniprot.org, 8680 entries) were performed with the Progenesis for Proteomics software (version 4.0, Waters). Peptides identification followed the parameters: maximum 1 missed cleavage site allowed for trypsin digestion; cysteine carbamidomethylation as fixed modification and methionine oxidation as variable

169 modification. The search for phosphopeptides was made through variable modification of
170 serine, threonine and tyrosine phosphorylation. Protein identification used the following
171 criteria: False discovery rate (FDR) set at less than 1%, minimum of 2 fragment ions per
172 peptide, 5 fragment ions per protein, and 2 peptides per protein. Relative protein quantification
173 was performed by the Hi-N approach, using the three most abundant peptides, with priority of
174 the unique peptides' ones (58). Normalized data were exported to Excel files.
175
176 *2.6 Pathway analysis*
177
178 The proteins differentially expressed and/or differentially phosphorylated among the
179 groups were included in the test to determine enriched pathways, using the online Panther
180 platform (http://www.pantherdb.org, version 14.1, released 2019-07-11). The whole *Rattus*
181 *norvegicus* proteome was used as the reference list and the Reactome Pathways was used as the
182 annotation data set. Significantly enriched pathways were based on Fisher's exact test followed
183 by Bonferroni correction with significance set to $p < 0.05$.
184
185 *2.7* RAT *fatty acid composition*
186
187 Aliquots of 1,000 mg of RAT were extracted in hexane/isopropanol (3:2 v/v) containing
188 0.01% butylated hydroxytoluene (BHT). After addition of chloroform/methanol/water (2:1:1
189 v/v/v), the samples were centrifuged (10,000 x g for 10 minutes) and the organic layers were
190 separated and evaporated to complete dryness with oxygen-free nitrogen (OFN). The lipids
191 were partitioned again in chloroform/methanol/water (8:4:3 v/v/v) and the chloroform layer
192 was dried under OFN.
193 Fatty acid analysis was performed as previously described (7). Briefly, fatty acid methyl
194 esters (FAME) were obtained by heating the samples with 15% acyl chloride in dry methanol
195 in a sealed tube at 70ºC during 3 hours under OFN. A solution of 5% NaCl was used to stop the
196 reaction, at room temperature, and FAMEs were extracted by 3 washings with petroleum ether
197 containing 0.01% BHT. Gas chromatography with flame ionization detector (GC2010 Plus,

Shimadzu, Kyoto, Japan) was performed with a TRACE TR-FAME capillary column (Thermo Scientific, Rockford, IL, USA). The intensity of peaks was quantified using the software Labsolutions (Shimadzu, Kyoto, Japan).

2.8 Statistical analysis

Body weight, white fat depots mass, and serum parameters variables were tested for normality (Shapiro-Wilk test) and homoscedasticity (Levene's test). Normally distributed variables (means ± standard error) were analyzed ANOVA and Tukey post hoc test. Non-parametric variables (median and interquartile range) were analyzed by Kruskal-Wallis ANOVA followed by two tailed multiple comparisons. All tests were performed with Statistica 12 Software (StatSoft, Tulsa, OK, USA) for $p < 0.05$.

Proteome and phosphoproteome data were submitted to analysis on the online platform MetaboAnalyst (http://www.metaboanalyst.ca). Data were log transformed and the missing values were replaced by half the minimum positive value in the original data. The data was normalized by pareto scaling and submitted to principal component analysis (PCA) followed by partial least-squares discriminant analysis (PLSDA). Variable importance for the projection (VIP) values higher than 1.5 in the principal component 1 were considered in order to identify the proteins and phosphopeptides that most contributed to discrimination among the groups.

3. Results

3.1 Ovariectomy induced high adiposity and insulin resistance

As shown in Table 1, the success of ovariectomy was confirmed by the low uterus weight of the ovariectomized groups. Initial body weight was similar among the 3 groups while both ovariectomized groups had higher body weights, feed efficiency and total fat mass at the end of the 12 weeks. Regarding the individual fat depots masses, while the gonadal fat depot was not different among the groups, both retroperitoneal and mesenteric depots were increased by

ovariectomy and not normalized by estrogen replacement. The elevations induced by ovariectomy in leptin and insulin levels, leptin/adiponectin ratio, HOMA-IR and HOMA-β were significantly attenuated by estradiol replacement. Total cholesterol, HDL-cholesterol and triglycerides levels did not differ significantly among the groups. RAT levels of TNF-α and IL-6 were similar among the groups.

3.2 Ovariectomy induced changes in protein expression and phosphorylation and modified metabolic pathways in retroperitoneal fat

Among the 18 biological samples, 13.722 peptides, corresponding to 1.246 proteins, were identified, of which 994 proteins met the inclusion criteria and were included in the statistical analysis. The multivariate analysis found 91 RAT proteins significantly modulated among the groups. The PLSDA analysis based on principal components showed a separation between the Sham and the Ovx groups while the Ovx+E2 group presented an intermediate profile (Figures 1A). Forty-two proteins were downregulated and 49 proteins were upregulated by ovariectomy, in relation to the Sham group. The E2-replacement group presented 43 downregulated proteins and 48 upregulated proteins, in comparison to the Sham group. The complete list of proteins with altered expression is presented in Appendix 1 (supplementary material).

Considering the phosphoproteome results, 1074 peptides were identified with at least one phosphorylation site, corresponding to 468 proteins. The multivariate analysis found 107 peptides (corresponding to 96 proteins) with a characteristic phosphorylation pattern for each group. The analysis based on principal components showed a separation of Sham and Ovx groups, while the replacement group showed to be in an intermediate position (Figures 1B). In comparison to the Sham group, the Ovx group showed decreased phosphorylation of 39 proteins and 68 proteins showed increased phosphorylation. The Ovx+E2 group showed downregulation of 42 proteins and 65 proteins with increased phosphorylation compared to Sham group. The complete list of proteins with altered phosphorylation is presented in Appendix 2 (supplementary material).

The pathway overrepresentation test showed significantly enrichment of pathways involved in lipid metabolism: fatty acyl-CoA biosynthesis pathway (1 protein/4 phosphopeptides; p = 2.67E-2) (Figure 2A) and metabolism of lipids pathway (9 proteins/11 phosphopeptides; p = 5.30E-5), the latter including fatty acid metabolism (6 proteins/9 phosphopeptides; p = 7.35E-8) and mitochondrial fatty acid β-oxidation (4 proteins/2 phosphopeptides; p = 1.65E-3) (Figure 2B). The proteins participating in these pathways included long-chain-fatty-acid-CoA ligase 5 (ACSL5), long-chain-fatty-acid-CoA ligase 1 (ACSL1), short-chain specific acyl-CoA dehydrogenase (ACADS), long- chain specific acyl-CoA dehydrogenase (ACADL), very long- chain specific acyl-CoA dehydrogenase (ACADVL), acyl-coenzyme A thioesterase type 2 (ACOT2), enoyl-CoA delta isomerase-1 (ECI1), acetyl-CoA carboxylase-1 (ACC1), and fatty acid synthase (FAS) (Table 2).

The innate immune metabolism pathway (10 proteins/16 phosphopeptides; p = 1.82E-7), including the neutrophil degranulation pathway (5 proteins/13 phosphopeptides; p = 2.07E-10), was also altered by ovariectomy (Figure 3), and the affected proteins included the platelet glycoprotein 4 (CD36). Two other important proteins related to the immune system were adenylyl cyclase-associated protein 1 (CAP1) and class I histocompatibility antigen, non-RT1.A alpha-1 chain (RT1-AW2) (Table 2).

The last two enriched pathways were the metabolism of vitamins and cofactors pathway (5 proteins/4 phosphopeptides; p = 4.29E-2) (Figure 4A) and the integration of energy metabolism pathway (3 proteins/6 phosphopeptides; p = 5.74E-4), which included the pathway ChREBP activates metabolic gene expression (3 phosphopeptides; p = 4.42E-2) (Figure 4B).

Table 2 also shows that ovariectomy induced changes in two proteins related to adipogenesis, all-trans-retinol 13,14-reductase (RETSAT) and lipoprotein lipase (LPL) as well as two proteins involved in insulin sensitivity, elongation factor 1-delta (EEF1D) and integrin-β1 (ITB1).

3.3 Ovariectomy increased saturated fatty acid content and disturbed the polyunsaturated fatty acid ratios in RAT

The results regarding the fatty acid analyses are depicted in Table 3. The Ovx group showed increased content of lauric, myristic and palmitic acids in relation to Sham. Increased total saturated fatty acids (SFA), alongside increased palmitic/stearic ratio, was also found in Ovx group. Estrogen replacement brought the content of lauric and myristic acids, as well as total SFA, back to levels comparable to Sham.

The monounsaturated fatty acids (MUFAs) myristoleic and palmitoleic acids levels were higher in Ovx group as compared to Sham, but comparable to Sham when estrogen replacement was introduced. Eicosenoic acid was lower in both Ovx and Ovx+E2 groups as compared to Sham. The palmitic/palmitoleic ratio was significantly decreased in Ovx, but normalized in Ovx+E2 group.

Ovariectomy led to a significant disturbance in the proportions of various polyunsaturated fatty acids (PUFAs). The essential fatty acids alpha-linoleic and linoleic acids were respectively increased and decreased in the Ovx group, as compared to the Sham group. Estrogen replacement was successful in returning linoleic acid back to a level comparable to Sham, but the same was not found for alpha-linolenic acid. A significant increase in eicopentaenoic acid (EPA) was found in Ovx and Ovx+E2 groups. An increase in arachidonic acid (AA) was also found in both groups, as compared to the Sham group, but such difference did not reach statistically significant levels.

Ovariectomy increased 0.33% of the total n-3 while decreasing 3% of the total n-6, in comparison to the Sham group. Such differences reached statistically significant levels, and whilst they remained for total n-3 in Ovx+E2 group, they were no longer statistically different for n-6 in Ovx+E2 group. The total n-6/n-3 ratio was lower in Ovx and Ovx+E2 groups, in comparison to the Sham group; however, the total SFA/PUFA ratio was higher in Ovx, and similar in Ovx+E2, when compared to Sham.

4. Discussion

Menopause has been considered as an important factor leading to obesity, mainly due to the shift in fat distribution from subcutaneous to visceral (24). We thus hypothesized that the

loss of ovarian hormones could lead to impairment of protein and lipid regulation in the visceral adipose tissue. In order to test this hypothesis, we used shotgun proteomics, along with fatty acid profiling, to determine proteins and lipids affected and to evaluate to what extent estrogen replacement would modify the ovariectomy-induced alterations.

In the rat, the visceral adipose tissue is comprised by the retroperitoneal, perirenal, perigonadal, and mesenteric depots (38). Ovariectomy has been shown to induce significant changes in RAT metabolism (1, 12, 49).

Ovariectomy increased body weight gain and adiposity due to increased feed efficiency, as food intake was not increased. Insulin and leptin levels, leptin/adiponectin ratio, and HOMA indexes also increased after ovariectomy and these alterations were attenuated by the estradiol replacement therapy, as we have previously shown (5). The estrogen replacement dose was chosen as to be compatible with the human dosage of the average transdermal replacement therapy for postmenopausal women (22, 48).

The pathway analyses indicated that the ovariectomy had a large impact on the metabolism of lipids, affecting fatty acid metabolism/mitochondrial fatty-acids β–oxidation pathway and the fatty acyl-CoA biosynthesis pathway. Figure 5 depicts the main effects of ovariectomy in these pathways, which will be addressed below.

The activation of free fatty acids by their association with coenzyme-A, yielding fatty-acyl CoA, is promoted by the ligases enzymes and represents a crucial step both for β-oxidation and synthesis of triacylglycerols and other lipids. In comparison to the Sham group, we observed down regulation of the protein ACSL5, a feature that has been associated with low β-oxidation rates (27), and increased phosphorylation of the protein (ACSL1). The present result on ACSL5 agrees with a previous report of its reduced gene expression in diabetic mice (32). The phosphorylation sites of the ACSL1 found in the present study (Thr^{27} and Thr^{40}) have not been reported previously while a threonine phosphorylation site (Thr^{85}) was described in liver mitochondria of normal rats under physiological conditions (13).

The acyl-CoA dehydrogenases, responsible for fatty acyl-CoA desaturation in the β-oxidation pathway (19), also showed an effect of ovariectomy. The protein ACADS showed downregulation in comparison to the Sham group. This is in accordance with a report in the

342 white adipose tissue from obese subjects (39). The ACADL and ACADVL proteins presented
343 increased phosphorylation (Ser^{210} and Ser^{418}, respectively), as compared to the Sham group.
344 While ACADVL has no phosphorylation sites previously reported, there is a previous
345 description of decreased serine phosphorylation of ACADL (Ser^{28}/Ser^{30}) after ischemia in
346 ovarian tumor grafts (41) and a demonstration that its decreased phosphorylation (Ser^{586}) in
347 fibrotic lung cells was associated with higher lipid peroxidation in comparison to normal lung
348 cells (24).
349 Two other enzymes of the mitochondrial fatty-acids β–oxidation pathway, ACOT2 and
350 ECI1, showed downregulation in response to ovariectomy. Located in the mitochondrial
351 matrix, ACOT2 targets mainly long-chain fatty acyl-CoAs and catalyzes their hydrolysis to the
352 free fatty acids and CoA. This mechanism has been proposed to enhance hepatic long-chain
353 fatty acids oxidation by preventing accumulation of fatty acyl-CoA during high rates of hepatic
354 β-oxidation (43, 61). ECI1 is involved in the process of oxidation of unsaturated fatty acids and
355 has been reported to be downregulated in white adipose tissue from Zucker diabetic-fatty
356 female rats (34).
357 Ovariectomy also affected proteins involved in fatty acids synthesis. The protein ACC1
358 showed decreased phosphorylation at Thr^{2278}, attenuated by estradiol replacement. ACC1
359 converts acetyl-CoA into malonyl-CoA during *de novo* lipogenesis. Although the
360 phosphorylation site found in the present study has not been previously described, the
361 phosphorylation of at least other five sites was demonstrated to inhibit the protein activity,
362 resulting in lower malonyl-CoA levels (25, 18). In addition, the protein FAS showed increased
363 phosphorylation at Ser^{725}, in comparison to the Sham group. FAS is a key enzyme in the
364 lipogenesis process, catalyzing the conversion of malonyl-CoA to palmitic acid (59). FAS
365 phosphorylation at Ser^{725} was increased in the liver of mice after re-feeding, a situation
366 favoring lipogenesis (65). Ovariectomy has been shown to increase FAS protein expression in
367 the retroperitoneal adipose tissue of rats (31). The present observation that the lipid metabolism
368 alterations induced by ovariectomy were attenuated by estradiol replacement agrees with a
369 report of decreased lipogenesis by estradiol through inhibition of ACC1 and FAS (37).

Ovariectomy also modulated proteins involved in the adipogenesis process. The protein RETSAT showed increased expression and decreased phosphorylation in comparison to the Sham group. This protein favors adipocyte differentiation under normal metabolic conditions and was shown to be induced during adipogenesis, being positively regulated by the transcription factor peroxisome proliferator activated receptor γ. Furthermore, the downregulation of the protein has been shown to inhibit adipogenesis (44, 57). Because the present Ovx animals showed increased body fat and mild increases in adipose tissue citokyne levels, it can be suggested that the upregulated RETSAT indicates a state of active fat accumulation. Moreover, further studies are necessary to elucidate the consequences of reduced phosphorylation of the sites found in the present study (Ser^{404}/Tyr^{409}).

The protein LPL showed increased expression and phosphorylation in the Ovx groups, as compared to the Sham group, indicating a high capacity of the retroperitoneal adipose tissue for uptake of lipoprotein-derived free fatty acids. This enzyme has also been implicated in adipocyte differentiation and it has shown increased expression in adipose-derived mesenchymal stem cells from ovariectomized mice (17). Moreover, estrogens have been shown to decrease LPL expression in the subcutaneous fat of premenopausal women (52). Of note, we were not able to find previous records of the phosphorylation site found in the present study (Tyr^{191}).

Since ovariectomized animals were obese and showed alterations in many proteins involved in lipid metabolism, we hypothesized that fatty acid composition of RAT could be affected. Data about the effects of ovariectomy-induced obesity on fatty acid profile are scarce, although the pro-inflammatory state of common obesity has been associated to SFA in the adipose tissue (10). Our results showed an increased palmitic acid and total SFA contents of RAT. Estrogen replacement was able to attenuate these effects. In postmenopausal obese women, visceral adipose tissue inflammation has been related to accumulation of SFA, especially palmitic acid (66). Although palmitic acid has been shown to impact fatty acids metabolism by upregulating the expression of ACSLs (47, 53), high levels have been found to lower fatty acid oxidation due to inhibition of carnitine-palmitoyltransferase 1A (34).

Ovariectomy also increased the percentage of the monounsaturated palmitoleic fatty acid. Endogenous non-dietary palmitoleic acid originates mainly from *de novo* lipogenesis in white adipose tissue, and has been recently considered as a lipokine, since it is released from the tissue and acts on distant cells. However, its metabolic effects have not been elucidated, as both deleterious and beneficial effects on adiposity, insulin sensitivity and lipid profile have been described (16). In the present study, its higher levels after ovariectomy are consistent with the proteomic results indicating a high lipogenesis rate, attenuated by estradiol replacement.

Regarding polyunsaturated fatty acids, our results showed a decrease in linoleic acid (n-6) and an increase in alpha-linolenic acid (n-3). Linoleic acid is a precursor of pro-inflammatory lipid mediators such as prostaglandins and leukotrienes (54). Although we did not measure these factors, it is fair to speculate that the decrease in linoleic acid in the ovariectomized animals was a consequence of its recruitment for the production of pro-inflammatory factors, since we had indications of an inflamed status induced by ovariectomy, as discussed above. Given the fact that the sum of PUFAs did not differ among the groups, the increase in n-3 was a direct consequence of the n-6 decrease.

These present findings indicate that ovariectomy favored a disruption of fat metabolism, which may have been relevant in the development of obesity. However, on the basis of our observations, it is not possible to rule out that, rather than a cause, the observed changes in lipid metabolism were a consequence of obesity.

The pathway analysis also showed that several proteins that take part in the innate immune system, which orchestrates inflammation (15), were modulated by ovariectomy. CD36 produced in macrophages is considered a pro-inflammatory marker. In the present study, this protein was upregulated by ovariectomy, in comparison to the Sham group, in agreement with findings in the visceral adipose tissue of postmenopausal women, obese individuals of both genres, and in the perivascular adipose tissue of diabetic rats (4, 30). CD36 is also involved in fatty acid translocation, thus influencing fat storage. Increased mRNA levels of CD36 in liver and visceral adipose tissue of ovariectomized mice has been associated with hepatic steatosis and increased visceral fat mass (50). Additionally, $CD36^{-/-}$ mice have shown enhanced fatty

426 acid oxidation measured in muscle cells lines (55). These data agree with the present
427 suggestion of impaired fatty acid oxidation in the visceral adipose tissue after ovariectomy.
428 Although not shown in the pathway analysis, it is relevant to notice two other proteins
429 altered by ovariectomy which have important inflammatory roles. The protein CAP1 showed
430 increased expression and phosphorylation, in comparison to the Sham group. In monocytes,
431 this protein was described to function as a receptor for adipocyte-derived resistin, which in turn
432 regulates inflammation signaling, leading to the release of pro-inflammatory cytokines. Its
433 expression was found to be increased in cells extracted from white adipose tissue of obese
434 humans (9). The phosphorylation at Thr^{306}/Ser^{307} identified in the present study were found to
435 be increased in response to lipopolyssacharide-induced inflammation in macrophages (29),
436 which corroborates the idea of an overall inflammatory status of our experimental model.
437 Moreover, the protein RT1-AW2 also showed increased expression and phosphorylation in
438 comparison to the Sham group. This protein is involved in immune response and was shown to
439 be upregulated in the secretome of hepatocytes of rats treated with hepato-carcinogenenic
440 substances, a condition also associated with a pro-inflammatory environment (64). The
441 phosphorylation site described in the present study (Ser^{295}) has not been described yet but the
442 Ser^{354} phosphorylation was found to be increased in liver mitochondria from obese mice (26).
443 Estrogen replacement attenuated the ovariectomy-induced changes regarding the proteins
444 CD36, CAP1 and RT1-AW2. These results are compatible with the increase in leptin levels as
445 well as a decrease in leptin/adiponectin ratio and suggest an overall effect of estrogen
446 replacement in reducing the inflammation status. This is compatible with reports that estradiol
447 may regulate cell recruitment to inflammatory sites and decrease the production of pro-
448 inflammatory cytokines, balancing the acute innate immune response (60).
449 Regarding the glucose metabolism impairment mentioned above, two proteins that play a
450 role in insulin resistance were shown to be modulated by ovariectomy. One of them is EEF1D,
451 which is involved in the protein elongation steps during the synthesis of a variety of proteins,
452 acting in the regulation of translation and transcription (56). Insulin stimulates the activity of
453 this enzyme, mainly through phosphorylation processes in adipose tissue, as observed after *in*
454 *vitro* experiments using adipose-derived cells 3T3-L1 (8). The fact that this protein showed

455 downregulated expression in the Ovx group, as compared to the Sham group, is compatible
456 with our suggestion of insulin resistance after ovariectomy. The other protein is ITB1, which
457 showed decreased expression and increased phosphorylation induced by ovariectomy, as
458 compared to the Sham group. The protein is localized in the cell membrane and participates in
459 the signaling between extracellular matrix and the intracellular environment, and dysfunctional
460 integrins have been related to insulin resistance (35). In visceral fat pads isolated from chow-
461 fed rats, ITB1 potentiated the ability of insulin to enhance tyrosine phosphorylation of insulin
462 receptor substrate 1 (21). Increased phosphorylation at Ser^{263} described in the present study has
463 been previously found in breast cancer, but the consequences of this cancer-induced alteration
464 on ITB1 function have not yet been explored (42). Since this modification appeared in the
465 present study in an obese pathological condition, it may be not inferred whether it yielded a
466 deleterious effect or, alternatively, whether it represented a counter-regulatory mechanism to
467 insulin resistance.
468
469 **5. Conclusion**
470 The present results indicate that ovariectomy favored lipogenesis while it impaired fatty
471 acids oxidation, and induced a pro-inflammatory state in the RAT. These effects are consistent
472 with the findings of high adiposity, hyperleptinemia, and impaired insulin sensitivity. The
473 observed alterations were partially attenuated by estradiol replacement. The data point to a role
474 of disrupted lipid metabolism in adipose tissue in the genesis of obesity after menopause.

Acknowledgements

The authors thank Mauro Cardoso Pereira for animal care, Nelson Inácio Pinto for assistance throughout the treatments and Debora Estadella for the contribution regarding Figure 4 creation.

Funding Statement

This study was financed by the Brazilian Agencies: Coordenação de Aperfeiçoamento de Pessoal de Nível Superior (CAPES, Finance Code 001), Conselho Nacional de Desenvolvimento Científico e Tecnológico (CNPq, Grants 453924/2014-0 and 309505/2017-8), and Fundação de Amparo à Pesquisa do Estado de São Paulo (FAPESP, Grant No. 2012/03172-4)

Conflict of Interests/ Financial Disclosure Statement

The authors certify that they comply with the ethical guidelines for authorship and publishing of the American Journal of Physiology Endocrinology and Metabolism. The authors declare that they have no conflict of interest, be it financial or not.

Author Contribution Statement

V.T.B. performed all experiments and wrote the manuscript
A.P.P. participated in all experiments and supervised results interpretation;
D.M.S. and C.BT. participated in the proteomic analyses and results interpretation;
E.G.L contributed to the statistical analyses and results interpretation;
A.A.B participated in the lipid profile analysis and results interpretation;
C.M.O.N. and L.M.O provided essential reagents and were responsible for Elisa assays*;*
E.B.R. supervised the whole project and the manuscript writing.

References

1. **Amengual-Cladera E, Lladó I, Gianotti M, Proenza AM**. Retroperitoneal white adipose tissue mitochondrial function and adiponectin expression in response to ovariectomy and 17β-estradiol replacement. *Steroids* 77(6):659-65, 2012. doi: 10.1016/j.steroids.2012.02.012.

2**. Amengual-Cladera E, et al**. Proteomic study of periovarian adipose tissue in 17β-estradiol-treated and untreated ovariectomized rats. *Biochem Cell Biol* 94(2):167-75, 2016. doi: 10.1139/bcb-2015-0077.

3. **Andersson T, Söderström I, Simonyté K, Olsson T**. Estrogen reduces 11beta-hydroxysteroid dehydrogenase type 1 in liver and visceral, but not subcutaneous, adipose tissue in rats. *Obesity* 18(3):470-5, 2010. doi: 10.1038/oby.2009.294.

4. **Azul L, Leandro A, Boroumand P, Klip A, Seiça R, Sena CM**. Increased inflammation, oxidative stress and a reduction in antioxidant defense enzymes in perivascular adipose tissue contribute to vascular dysfunction in type 2 diabetes. *Free Radic Biol Med*; 146:264-274, 2020. doi: 10.1016/j.freeradbiomed.2019.11.002.

5. **Boldarine VT, et al.** High-fat diet intake induces depressive-like behavior in ovariectomized rats. *Sci Rep* 22; 9(1):10551, 2019. doi: 10.1038/s41598-019-47152-1.

6. **Bueno AA, et al.** Long chain saturated fatty acids increase haptoglobin gene expression in C57BL/6J mice adipose tissue and 3T3-L1 cells. *Eur J Nutr* 49(4):235-41, 2010. doi: 10.1007/s00394-009-0069-z.

7. **Bueno AA, et al.** Dimethyl acetals, an indirect marker of the endogenous antioxidant plasmalogen level, are reduced in blood lipids of Sudanese pre-eclamptic subjects whose background diet is high in carbohydrate. *J Obstet Gynaecol* 32(3):241-6, 2012. doi: 10.3109/01443615.2011.641622.

8. **Chang YW, Traugh JA.** Insulin stimulation of phosphorylation of elongation factor 1 (eEF-1) enhances elongation activity. *Eur J Biochem* 251(1-2):201–207, 1998. doi:10.1046/j.1432-1327.1998.2510201.x

9. **Choi MS, et al.** High-fat diet decreases energy expenditure and expression of genes controlling lipid metabolism, mitochondrial function and skeletal system development in the adipose tissue, along with increased expression of extracellular matrix remodelling- and inflammation-related genes. *Br J Nutr* 113(6):867–877, 2015. doi:10.1017/S0007114515000100.

10. **Cusi K.** The role of adipose tissue and lipotoxicity in the pathogenesis of type 2 diabetes. *Curr Diab Rep* 10(4):306-15, 2010. doi:10.1007/s11892-010-0122-6.

11. **Dalal PK, Agarwal M.** Postmenopausal syndrome. *Indian J Psychiatry* 57:S222-32, 2015. doi: 10.4103/0019-5545.161483.

12. **de Souza CF, et al.** Estradiol protects against ovariectomy-induced susceptibility to the anabolic effects of glucocorticoids in rats. *Life Sci* 218:185-196, 2019. doi:10.1016/j.lfs.2018.12.037

13. **Distler AM, Kerner J, Hoppel CL.** Post-translational modifications of rat liver mitochondrial outer membrane proteins identified by mass spectrometry. *Biochim Biophys Acta* 1774(5):628-36, 2007.

14. **Dornellas APS et al.** High-Fat Feeding Improves Anxiety-Type Behavior Induced by Ovariectomy in Rats. *Front Neurosci* 12:557, 2018. doi: 10.3389/fnins.2018.00557.

15. **Eaton SA, Sethi JK.** Immunometabolic Links between Estrogen, Adipose Tissue and Female Reproductive Metabolism. *Biology* (Basel) 7;8(1). pii: E8, 2019. doi: 10.3390/biology8010008.

16. **Frigolet ME, Gutiérrez-Aguilar R.** The Role of the Novel Lipokine Palmitoleic Acid in Health and Disease. *Adv Nutr* 8(1):173S–181S, 2017. doi:10.3945/an.115.011130.

552 17. **Fu Y, et al.** Adipogenic differentiation potential of adipose-derived mesenchymal stem
553 cells from ovariectomized mice. *Cell Prolif* 47(6):604–614, 2014. doi:10.1111/cpr.12131.

554 18. **Galic S, et al.** AMPK signaling to acetyl-CoA carboxylase is required for fasting- and cold-
555 induced appetite but not thermogenesis. *Elife* 13;7. pii: e32656, 2018. doi:10.7554/eLife.32656.

556 19. **Ghisla S, Thorpe C.** Acyl-CoA dehydrogenases. A mechanistic overview. *Eur J Biochem*
557 271(3):494-508, 2004.

558 20. **Goettems-Fiorin PB, et al.** Ovariectomy predisposes female rats to fine particulate matter
559 exposure's effects by altering metabolic, oxidative,pro-inflammatory, and heat-shock protein
560 levels. *Environ Sci Pollut Res Int* 26(20):20581-20594, 2019. doi: 10.1007/s11356-019-05383-
561 9.

562 21. **Guilherme A, Torres K, Czech MP.** Cross-talk between insulin receptor and integrin
563 alpha5 beta1 signaling pathways. *J Biol Chem* 273(36):22899–22903, 1998.
564 doi:10.1074/jbc.273.36.22899.

565 22. **Hill DA, Crider M, Hill SR.** Hormone Therapy and Other Treatments for Symptoms of
566 Menopause. *Am Fam Physician* 94(11):884-889, 2016.

567 23. **Horber FF, et al.** Effect of sex and age on bone mass, body composition and fuel
568 metabolism in humans. *Nutrition* 13(6):524-34, 1997.

569 24. **Kabuyama Y, et al.** Dysregulation of very long chain acyl-CoA dehydrogenase coupled
570 with lipid peroxidation. *Am J Physiol Cell Physiol* 298(1):C107-13, 2010. doi:
571 10.1152/ajpcell.00231.2009.

572 25. **Kim KH, et al.** Role of reversible phosphorylation of acetyl-CoA carboxylase in long-
573 chain fatty acid synthesis.*FASEB J* 3(11):2250-6, 1989.

574 26. **Klepeisz P, et al.** Phenobarbital induces alterations in the proteome of hepatocytes and
575 mesenchymal cells of rat livers. *PLoS One* 8(10):e76137, 2013.
576 doi:10.1371/journal.pone.0076137.

577 27. **Knights KM.** Role of hepatic fatty acid:coenzyme A ligases in the metabolism
578 ofxenobiotic carboxylic acids. *Clin Exp Pharmacol Physiol* 25(10):776-82, 1998.

579 28. **Kozakowski J, et al.** Obesity in menopause -our negligence or an unfortunate inevitability?
580 *Prz Menopauzalny* 16(2):61-65, 2017. doi: 10.5114/pm.2017.68594.

581 29. **Lee S, et al**. Adenylyl cyclase-associated protein 1 is a receptor for human resistin and
582 mediates inflammatory actions of human monocytes. *Cell Metab* 19(3):484–497, 2014.
583 doi:10.1016/j.cmet.2014.01.013.

584 30. **Lesna IK, et al.** Human adipose tissue accumulation is associated with pro-inflammatory
585 changes in subcutaneous rather than visceral adipose tissue. *Nutr Diabetes* 10;7(4): e264, 2017.
586 doi: 10.1038/nutd.2017.15.

587 31. **Leu SY, et al.** Raspberry ketone reduced lipid accumulation in 3T3-L1 cells and
588 ovariectomy-induced obesity in Wistar rats by regulating autophagy mechanisms. *J Agric Food*
589 *Chem* 20;65(50):10907-10914, 2017. doi: 10.1021/acs.jafc.7b03831.

590 32. **Lewin TM, et al.** Acyl-CoA synthetase isoforms 1, 4 and 5 are present in different
591 subcellular membranes in rat liver and can be inhibited independently. *J Biol Chem*. 276
592 (24674-24679), 2001.

593 33. **Li P, et al.** Effect of non-esterified fatty acids on fatty acid metabolism-related genes in calf
594 hepatocytes cultured in vitro. *Cell Physiol Biochem* 32(5):1509-16, 2013. doi:
595 10.1159/000356588.

596 34**.Liang Y, She P, Wang X, Demarest K.** The messenger RNA profiles in liver,
597 hypothalamus, white adipose tissue, and skeletal muscle of female Zucker diabetic fatty rats
598 after topiramate treatment. *Metabolism* 55(10):1411-9, 2006.

599 35. **Lin D, Chun TH, Kang L.** Adipose extracellular matrix remodelling in obesity and insulin
600 resistance. *Biochem Pharmacol* 119:8–16, 2016. doi:10.1016/j.bcp.2016.05.005.

601 36. **Lin Y, et al.** Sodium laurate, a novel protease- and mass spectrometry-compatible detergent
602 for mass spectrometry-based membrane proteomics. *PLoS One* 8(3):e59779, 2013. doi:
603 10.1371/journal.pone.0059779.

604 37. **López M, Tena-Sempere M**. Estradiol effects on hypothalamic AMPK and BAT
605 thermogenesis: A gateway for obesity treatment? *Pharmacol Ther* 178:109-122, 2017. doi:
606 10.1016/j.pharmthera.2017.03.014.

607 38. **Luong Q, Huang J, Lee KY**. Deciphering White Adipose Tissue Heterogeneity. *Biology*
608 *(Basel)*, 8(2):23, 2019. doi:10.3390/biology8020023.

609 39. **Marrades MP, et al**. Orchestrated downregulation of genes involved in oxidative
610 metabolic pathways in obese vs. lean high-fat young male consumers. *J Physiol Biochem*
611 67(1):15-26, 2011. doi: 10.1007/s13105-010-0044-4.

612 40. **Mathis D, Shoelson SE.** Immunometabolism: an emerging frontier. *Nat Rev Immunol*
613 11(2):81, 2011. doi: 10.1038/nri2922.

614 41. **Mertins P, et al.** Ischemia in tumors induces early and sustained phosphorylation changes
615 in stress kinase pathways but does not affect global protein levels. *Mol Cell Proteomics*
616 13(7):1690-704, 2014. doi: 10.1074/mcp.M113.036392.

617 42. **Mertins P, et al.** Proteogenomics connects somatic mutations to signalling in breast cancer.
618 *Nature* 534(7605):55–62, 2016. doi:10.1038/nature18003.

619 43. **Moffat C, et al.** Acyl-CoA thioesterase-2 facilitates mitochondrial fatty acid oxidation in
620 the liver. *J Lipid Res* 55(12):2458-70, 2014. doi: 10.1194/jlr.M046961.

621 44. **Moise AR, Kuksa V, Imanishi Y, Palczewski K.** Identification of all-trans-retinol:all-
622 trans-13,14-dihydroretinol saturase. *J Biol Chem* 279(48):50230–50242, 2004.
623 doi:10.1074/jbc.M409130200.

624 45. **Monteiro R, Teixeira D, Calhau C.** Estrogen signaling in metabolic inflammation.
625 *Mediators Inflamm* 2014:615917, 2014. doi: 0.1155/2014/615917.

626 46. **Moreno MF, et al.** Metabolic profile response to administration of epigallocatechin-3-
627 gallate in high-fat-fed mice. *Diabetol Metab Syndr* 6(1):84, 2014. doi: 10.1186/1758-5996-6-
628 84.

629 47. **Nakakuki M, Kawano H, Notsu T, Imada K.** Eicosapentaenoic acid suppresses
630 palmitate-induced cytokine production by modulating long-chain acyl-CoA synthetase 1
631 expression in human THP-1 macrophages. *Atherosclerosis* 227(2):289-96, 2013. doi:
632 10.1016/j.atherosclerosis.2012.12.036.

633 48. **Nair AB, Jacob S.** A simple practice guide for dose conversion between animals and
634 human. *J Basic Clin Pharm* 7(2):27-31, 2016. doi:10.4103/0976-0105.177703

635 49. **Neto NI, et al.** A Hyperlipidic Diet Combined with Short-Term Ovariectomy Increases
636 Adiposity and Hyperleptinemia and Decreases Cytokine Content in Mesenteric Adipose
637 Tissue. *Mediators Inflamm* 2015:923248, 2015. doi:10.1155/2015/923248

638 50. **Nishio E, et al.** Lack of association of ovariectomy-induced obesity with overeating and the
639 reduction of physical activities. *Biochem Biophys Rep* 8;20:100671, 2019. doi:
640 10.1016/j.bbrep.2019.100671.

641 51. **Pasing Y, Colnoe S, Hansen T.** Proteomics of hydrophobic samples: Fast, robust and low-
642 cost workflows for clinical approaches. *Proteomics*.; Mar; 17(6), 2017. doi:
643 10.1002/pmic.201500462.

644 52. **Price TM, et al.** Estrogen regulation of adipose tissue lipoprotein lipase--possible
645 mechanism of body fat distribution. *Am J Obstet Gynecol* 178(1 Pt 1):101–107, 1998.
646 doi:10.1016/s0002-9378(98)70634-9.

647 53. **Rajkumar A, et al.** ACSL5 genotype influence on fatty acid metabolism: a cellular, tissue,
648 and whole-body study. *Metabolism* 83:271-279, 2018. doi: 10.1016/j.metabol.2018.03.019.

649 54. **Robichaud PP, Surette ME.** Polyunsaturated fatty acid-phospholipid remodeling and
650 inflammation. *Curr Opin Endocrinol Diabetes Obes* 22(2):112-8, 2015.

651 55. **Samovski D, et al.** Regulation of AMPK activation by CD36 links fatty acid uptake to β-
652 oxidation. *Diabetes* 64(2):353-359, 2015. doi:10.2337/db14-0582.

653 56. **Sanders J, Raggiaschi R, Morales J, Möller W**. The human leucine zipper-containing
654 guanine-nucleotide exchange protein elongation factor-1 delta. *Biochim Biophys Acta*
655 1174(1):87–90, 1993. doi:10.1016/0167-4781(93)90097-w

656 57. **Schupp M, et al.** Retinol saturase promotes adipogenesis and is downregulated in obesity
657 [published correction appears in Proc Natl Acad Sci U S A. 2009 Mar 17;106(11):4571. Suh,
658 Moojin [corrected to Suh, Moo-Jin]]. *Proc Natl Acad Sci* 106(4):1105–1110, 2009.
659 doi:10.1073/pnas.0812065106.

660 58. **Silva JS, et al**. Quantitative proteomic analysis by accurate mass retention time pairs. *Anal*
661 *Chem* 77(7): 2187-2200, 2005. doi: 10.1021/ac048455k.

662 59. **Solinas G, Borén J, Dulloo AG.** De novo lipogenesis in metabolic homeostasis: More
663 friend than foe? *Mol Metab* 4(5):367-77, 2015. doi:10.1016/j.molmet.2015.03.004.

664 60. **Stubelius A, Andersson A, Islander U, Carlsten H.** Ovarian hormones in innate
665 inflammation. *Immunobiology* 222(8-9):878-883, 2017. doi: 10.1016/j.imbio.2017.05.007.

666 61. **Tillander V, Alexson SEH, Cohen DE.** Deactivating Fatty Acids: Acyl-CoA Thioesterase-
667 Mediated Control of Lipid Metabolism. *Trends Endocrinol Metab* 28(7):473-484, 2017. doi:
668 0.1016/j.tem.2017.03.001.

669 62. **Trujillo ME, Scherer PE.** Adipose tissue-derived factors: impact on health and disease.
670 *Endocr Rev* 27(7):762-78, 2006. doi: 10.1210/er.2006-0033.

671 63. **Weijers RN.** Lipid composition of cell membranes and its relevance in type 2 diabetes
672 mellitus. *Curr Diabetes Rev* 8(5):390-400, 2012. doi: 10.2174/157339912802083531.

673 64. **Weintz G, et al.** The phosphoproteome of toll-like receptor-activated macrophages. *Mol*
674 *Syst Biol* 6:371, 2010. doi:10.1038/msb.2010.29.

675 65. **Wilson-Grady JT, Haas W, Gygi SP.** Quantitative comparison of the fasted and re-fed
676 mouse liver phosphoproteomes using lower pH reductive dimethylation. *Methods* 61(3):277-
677 86, 2013. doi: 10.1016/j.ymeth.2013.03.031.

678 66. **Yamatani H, et al.** Association of estrogen with glucocorticoid levels in visceral fat in
679 postmenopausal women. *Menopause*. 20(4):437-42, 2013. doi:
680 10.1097/gme.0b013e318271a640.
681 67. **Yamatani H, et al.** Differences in the fatty acid metabolism of visceral adipose tissue in
682 postmenopausal women. *Menopause* 21(2):170-6, 2014. doi:
683 10.1097/GME.0b013e318296431a.

Figure legends

FIGURE 1: Separation of the groups using multivariate analyses of proteome data

(A) - Supervised PLSDA analyses based on 994 protein intensities. The principal components explaining the separation are 1 and 4; Q2=0.7; R2=0.9. **(B)** - Supervised PLSDA analyses based on 1074 peptide intensities. The principal components explaining the separation are 1 and 2; Q2= 0.6; R2= 0.9.

FIGURE 2: Representation of the innate immune metabolism pathway significantly and their associated proteins and phosphopeptides

Pathway enrichment analysis: Fisher's exact test followed by Bonferroni correction. The colored bars indicate the proteins expression/phosphorylation peak intensities. All 6 samples in each experimental group were included in the analyses

FIGURE 3: Representation of the fatty acyl-CoA biosynthesis (A) and metabolism of lipids (B) pathways and their associated proteins and phosphopeptides

Pathway enrichment analysis: Fisher's exact test followed by Bonferroni correction. The colored bars indicate the proteins expression/phosphorylation peak intensities. All 6 samples in each experimental group were included in the analyses

FIGURE 4: Representation of the metabolism of vitamins and cofactors (A) and integration of energy metabolism (B) pathways and their associated proteins and phosphopeptides

Pathway enrichment analysis: Fisher's exact test followed by Bonferroni correction. The colored bars indicate the proteins expression/phosphorylation peak intensities. All 6 samples in each experimental group were included in the analyses

FIGURE 5: Summary of the alterations in lipid metabolism induced by ovariectomy, as indicated by the proteome/phosphoproteome analysis

Red triangles indicate reduced protein expression; Arrows followed by amino acid symbol indicate reduced (↓) or increased (↑) phosphorylation of the residue in the protein shown. ACSL5: Long-chain fatty acid-CoA ligase 5; ACSL1: Long-chain fatty acid-CoA ligase 1; ACADS: Short-chain specific acyl-CoA dehydrogenase; ACADL: Long-chain specific acyl-CoA dehydrogenase; ACADVL: Very long-chain specific acyl-CoA dehydrogenase; ACOT2: Acyl-Coenzyme A thiosterase typ2; ECI1: Enoyl-CoA delta isomerase-1; ACC1: Acetyl-CoA carboxylase-1; FAS: Fatty acid synthase.

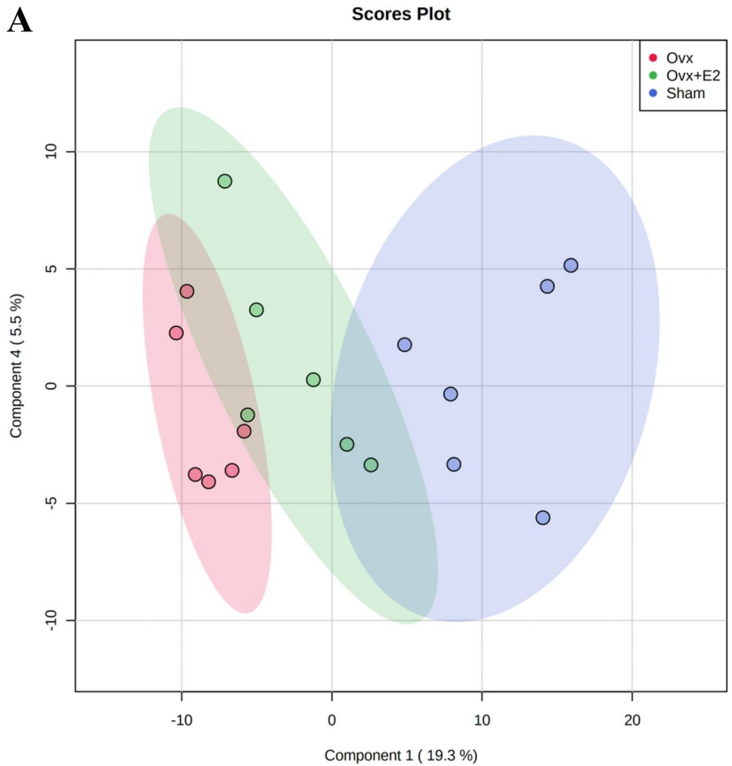
A
Scores Plot
Ovx
Ovx+E2
Sham
Component 4 (5.5 %)
Component 1 (19.3 %)
10
5
0
-5
-10
-10
0
10
20

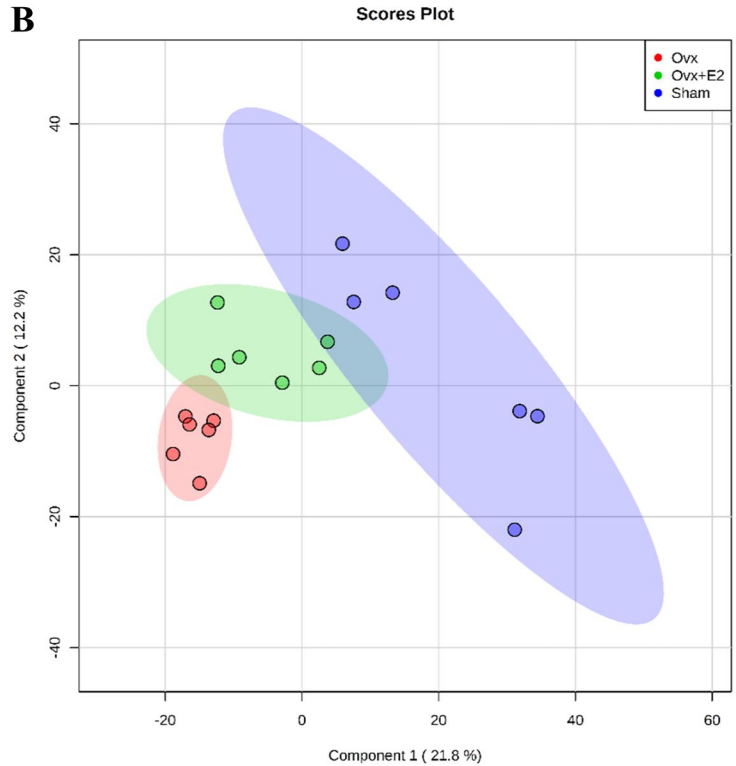
B
Scores Plot
Ovx
Ovx+E2
Sham
Component 2 (12.2 %)
Component 1 (21.8 %)
40
20
0
-20
-40
-20
0
20
40
60

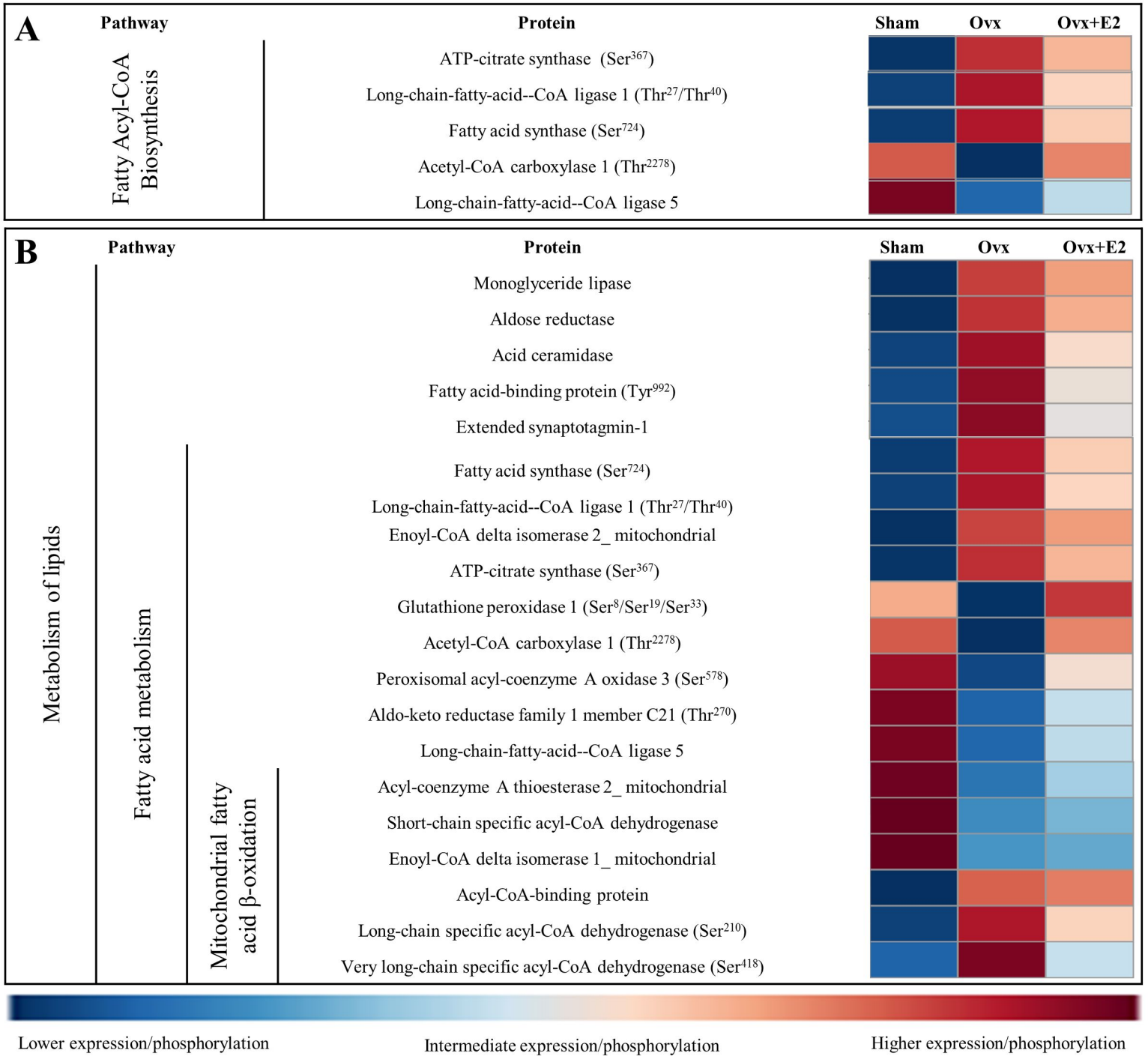
A
Pathway
Protein
Sham
Ovx
Ovx+E2
Fatty Acyl-CoA Biosynthesis
ATP-citrate synthase (Ser367)
Long-chain-fatty-acid--CoA ligase 1 (Thr27/Thr40)
Fatty acid synthase (Ser724)
Acetyl-CoA carboxylase 1 (Thr2278)
Long-chain-fatty-acid--CoA ligase 5
B
Pathway
Protein
Sham
Ovx
Ovx+E2
Metabolism of lipids
Fatty acid metabolism
Mitochondrial fatty acid β-oxidation
Monoglyceride lipase
Aldose reductase
Acid ceramidase
Fatty acid-binding protein (Tyr992)
Extended synaptotagmin-1
Fatty acid synthase (Ser724)
Long-chain-fatty-acid--CoA ligase 1 (Thr27/Thr40)
Enoyl-CoA delta isomerase 2_ mitochondrial
ATP-citrate synthase (Ser367)
Glutathione peroxidase 1 (Ser8/Ser19/Ser33)
Acetyl-CoA carboxylase 1 (Thr2278)
Peroxisomal acyl-coenzyme A oxidase 3 (Ser578)
Aldo-keto reductase family 1 member C21 (Thr270)
Long-chain-fatty-acid--CoA ligase 5
Acyl-coenzyme A thioesterase 2_ mitochondrial
Short-chain specific acyl-CoA dehydrogenase
Enoyl-CoA delta isomerase 1_ mitochondrial
Acyl-CoA-binding protein
Long-chain specific acyl-CoA dehydrogenase (Ser210)
Very long-chain specific acyl-CoA dehydrogenase (Ser418)
Lower expression/phosphorylation
Intermediate expression/phosphorylation
Higher expression/phosphorylation

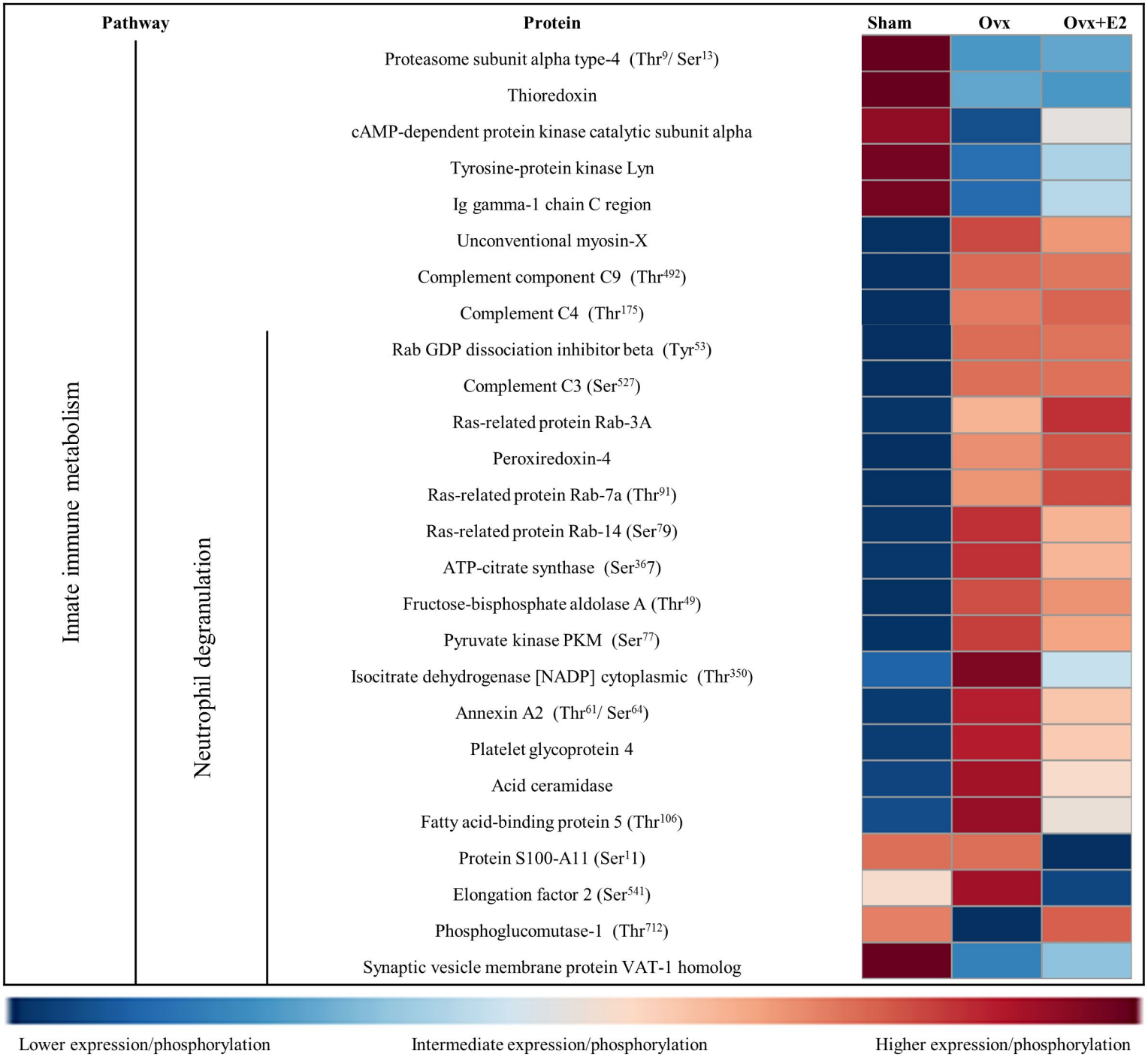
Pathway
Protein
Sham
Ovx
Ovx+E2
Innate immune metabolism
Neutrophil degranulation
Proteasome subunit alpha type-4 (Thr9/ Ser13)
Thioredoxin
cAMP-dependent protein kinase catalytic subunit alpha
Tyrosine-protein kinase Lyn
Ig gamma-1 chain C region
Unconventional myosin-X
Complement component C9 (Thr492)
Complement C4 (Thr175)
Rab GDP dissociation inhibitor beta (Tyr53)
Complement C3 (Ser527)
Ras-related protein Rab-3A
Peroxiredoxin-4
Ras-related protein Rab-7a (Thr91)
Ras-related protein Rab-14 (Ser79)
ATP-citrate synthase (Ser3677)
Fructose-bisphosphate aldolase A (Thr49)
Pyruvate kinase PKM (Ser77)
Isocitrate dehydrogenase [NADP] cytoplasmic (Thr350)
Annexin A2 (Thr61/ Ser64)
Platelet glycoprotein 4
Acid ceramidase
Fatty acid-binding protein 5 (Thr106)
Protein S100-A11 (Ser11)
Elongation factor 2 (Ser541)
Phosphoglucomutase-1 (Thr712)
Synaptic vesicle membrane protein VAT-1 homolog
Lower expression/phosphorylation
Intermediate expression/phosphorylation
Higher expression/phosphorylation

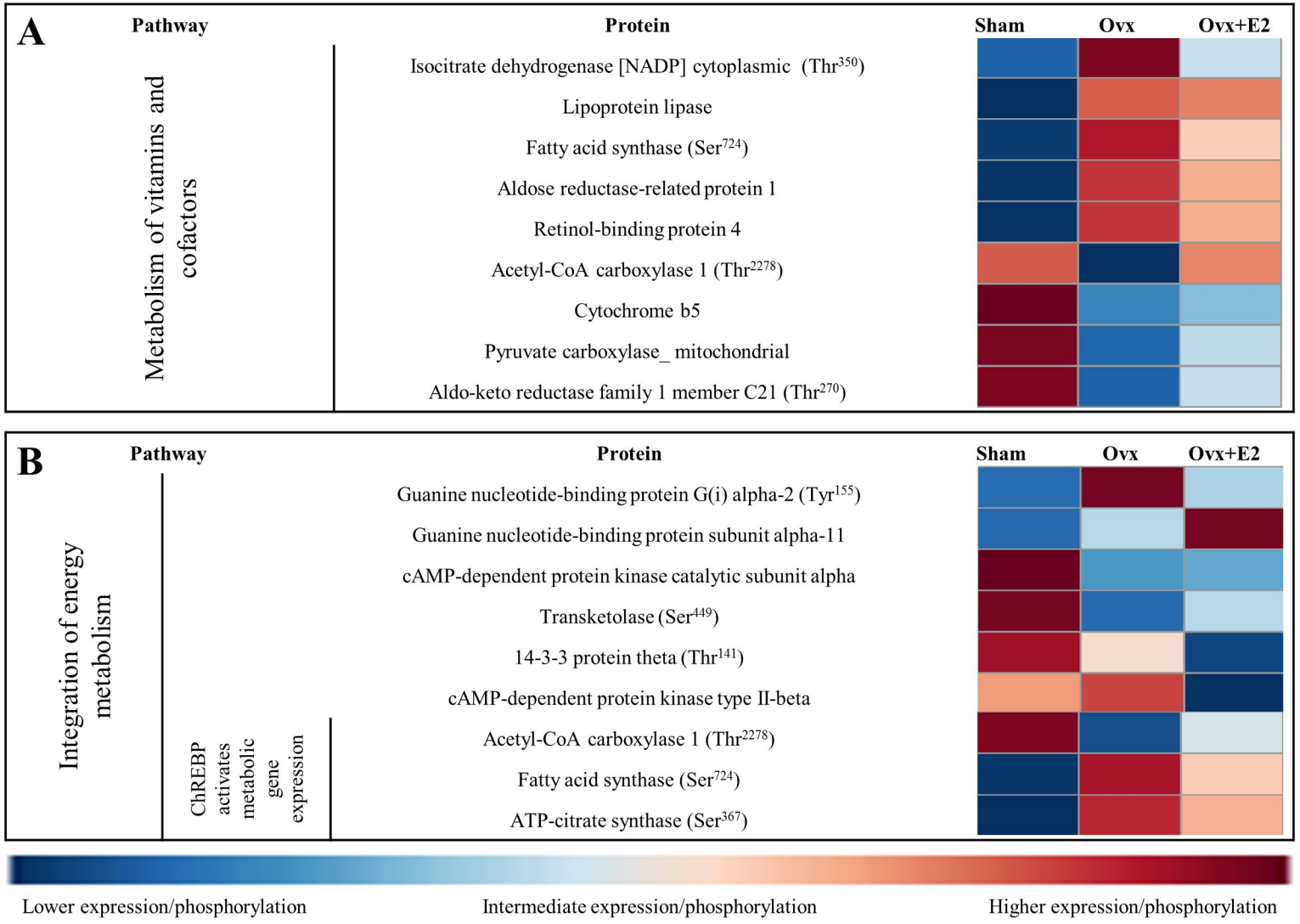
A
Pathway
Protein
Sham
Ovx
Ovx+E2
Metabolism of vitamins and cofactors
Isocitrate dehydrogenase [NADP] cytoplasmic (Thr350)
Lipoprotein lipase
Fatty acid synthase (Ser724)
Aldose reductase-related protein 1
Retinol-binding protein 4
Acetyl-CoA carboxylase 1 (Thr2278)
Cytochrome b5
Pyruvate carboxylase_ mitochondrial
Aldo-keto reductase family 1 member C21 (Thr270)
B
Pathway
Protein
Sham
Ovx
Ovx+E2
Integration of energy metabolism
ChREBP activates metabolic gene expression
Guanine nucleotide-binding protein G(i) alpha-2 (Tyr155)
Guanine nucleotide-binding protein subunit alpha-11
cAMP-dependent protein kinase catalytic subunit alpha
Transketolase (Ser449)
14-3-3 protein theta (Thr141)
cAMP-dependent protein kinase type II-beta
Acetyl-CoA carboxylase 1 (Thr2278)
Fatty acid synthase (Ser724)
ATP-citrate synthase (Ser367)
Lower expression/phosphorylation
Intermediate expression/phosphorylation
Higher expression/phosphorylation

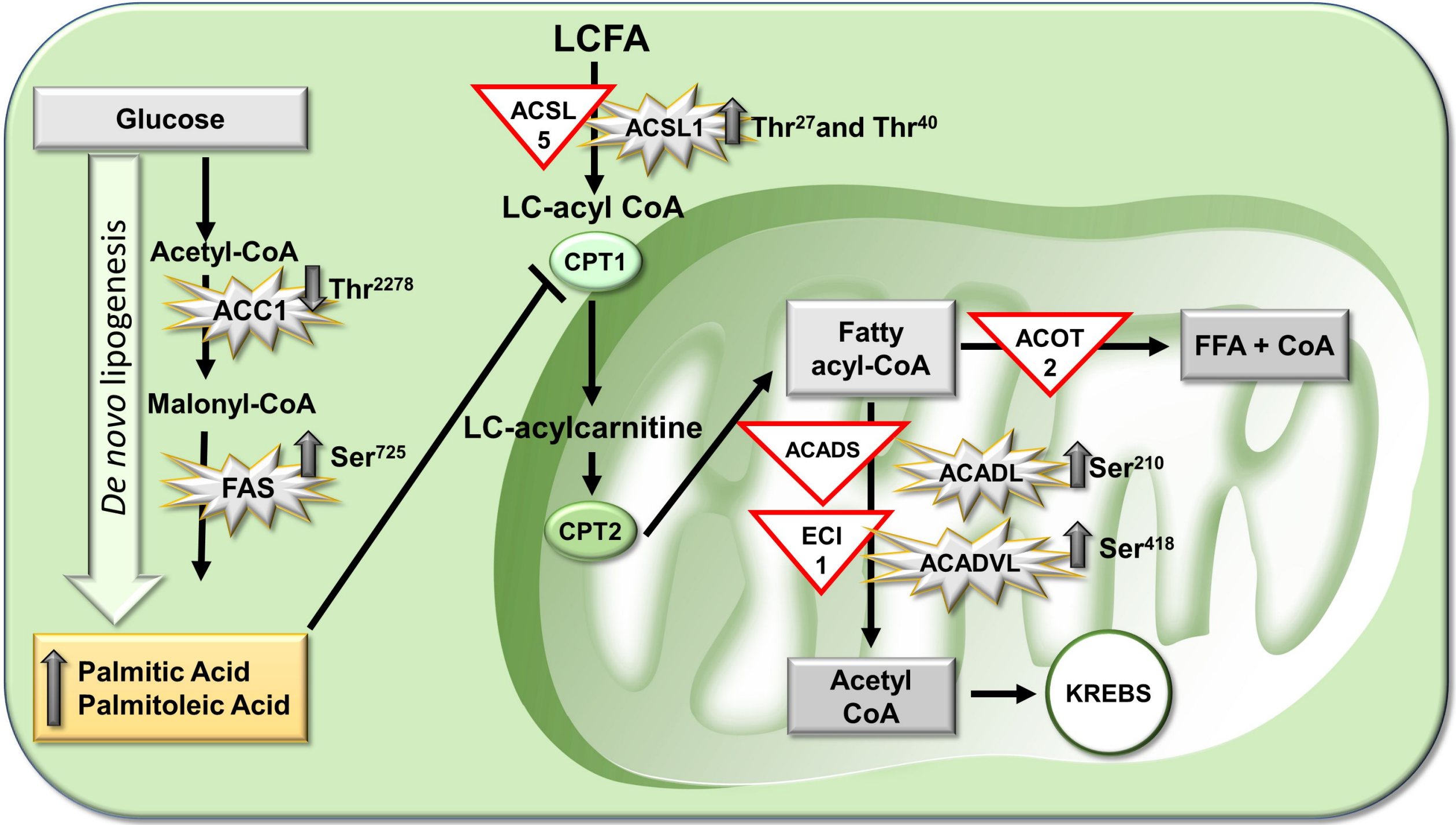
LCFA
ACSL 5
ACSL1
Thr27and Thr40
LC-acyl CoA
CPT1
Glucose
Acetyl-CoA
ACC1
Thr2278
Malonyl-CoA
FAS
Ser725
De novo lipogenesis
Palmitic Acid
Palmitoleic Acid
LC-acylcarnitine
CPT2
Fatty acyl-CoA
ACOT 2
FFA + CoA
ACADS
ACADL
Ser210
ECI 1
ACADVL
Ser418
Acetyl CoA
KREBS

Table 1: Body and serum parameters

	Sham	Ovx	Ovx+E2
Initial body weight (g)	264.79 ± 5.22	263.00 ± 3.79	263.51 ± 5.02
Final body weight (g)	280.84 (272.38 - 285.75)	338.00 (336.00 - 339.50)*	335.71 (325.89 - 337.00)*
Cumulative food intake (Kcal)	526.36 ± 14.87	570.90 ± 12.48	613.63 ± 13.01*
Feed efficiency (g/Kcal)	2.72 ± 0.54	13.52 ± 0.66*	11.98 ± 0.81*
Uterus (g)	0.43 ± 0.03	0.11 ± 0.02*	0.15 ± 0.02*
Total fat mass (g)	10.37 ± 0.89	17.71 ± 1.22*	15.89 ± 1.11*
Retroperitoneal fat mass (g)	3.49 ± 0.30	7.23 ± 0.56*	6.02 ± 0.46*
Mesenteric fat mass (g)	1.67 ± 0.17	3.75 ± 1.20*	3.38 ± 0.80*
Periovarian fat mass (g)	4.97 ± 0.44	6.15 ± 0.48	5.98 ± 0.49
Leptin (ng/mL)	2.17 (1.84 - 2.61)	10.06 (7.80-012.52)*#	5.97 (4.45 - 9.89)
Adiponectin (µg/mL)	5.65 ± 0.59	8.06 ± 1.04	7.67 ± 0.91
Leptin/Adiponectin	0.41 ± 0.06	1.42 ± 0.29*#	0.89 ± 0.18
TNF-α (pg/mg of protein)	7.04 ± 0.72	7.45 ± 0.78	6.96 ± 2.34
IL-6 (pg/mg of protein)	32.2 ± 5.28	54.6 ± 17.3	26.8 ± 2.62
Glucose (mg/dL)	92.80 ± 2.98	105.72 ± 6.38	103.88 ± 6.29
Insulin (ng/mL)	0.56 ± 0.06	2.32 ± 0.20*#	1.31 ± 0.12*
HOMA-IR	3.18 (2.32 - 4.25)	14.37 (12.08 - 19.07)*#	7.93 (6.26 - 8.28)
HOMA-β	0.18 (0.14 - 0.23)	0.52 (0.38 - 0.72)*#	0.29 (0.24 - 0.45)
Total cholesterol (mg/dL)	115.46 (104.96 - 121.76)	140.84 (119.08 - 193.13)	126.34 (119.85 - 133.97)
HDL cholesterol (mg/dL)	205.73 (179.01 - 251.91)	163.17 (146.18 - 174.05)	142.37 (135.50 - 157.63)
Triglycerides (mg/dL)	99.18 (94.67 - 108.20)	111.27 (105.33 - 118.85)	122.54 (107.79 - 220.49)

Data presented as mean ± SEM for variables with normal distribution or median-interquartile range (Q1-Q3) for variables not normally distributed. n=6 animals per group. * $p < 0.05$ vs Sham; # $p < 0.05$ vs Ovx+E2.

Table 2: Highlighted proteins with altered expression and/or phosphorylation

Protein (Phosphosite)	Expression fold-change			Phosphorylation fold-change		
	Ovx/Sham	Ovx+E2/Sham	Ovx+E2/Ovx	Ovx/Sham	Ovx+E2/Sham	Ovx+E2/Ovx
Long-chain-fatty-acid-CoA ligase 5	0.61	0.72	1.18			
Long-chain-fatty-acid-CoA ligase 1 (Thr^{27}/Thr^{40})				3.79	2.26	0.60
Short-chain specific acyl-CoA dehydrogenase, mitochondrial	0.59	0.63	1.06			
Long-chain specific acyl-CoA dehydrogenase, mitochondrial (Ser^{210})				27.25	7.84	0.29
Very long-chain specific acyl-CoA dehydrogenase, mitochondrial (Ser^{418})				4.49	1.75	0.39
Acyl-coenzyme A thioesterase 2, mitochondrial	0.62	0.70	1.13			
Enoyl-CoA delta isomerase 1, mitochondrial	0.54	0.56	1.03			
Acetyl-CoA carboxylase (Thr^{2278})				0.12	0.84	7.21
Fatty acid synthase (Ser^{725})				2.82	1.95	0.69
All-trans-retinol 13,14-reductase (Ser^{404}/Tyr^{409})	1.75	1.52	0.87	0.96	2.95	3.08
Lipoprotein lipase (Tyr^{191})	2.15	2.03	0.94	1.78	1.04	0.58
Platelet glycoprotein 4	1.53	1.33	0.86			
Adenylyl cyclase-associated protein 1 (Ser^{300}/Thr^{306}/Ser^{307})	2.12	1.01	0.47	18.49	1.20	0.07
Class I histocompatibility antigen, Non-RT1.A alpha-1 chain (Ser^{295})	12.80	2.61	0.20	12.79	2.35	0.18
Elongation factor 1-delta (Ser^{447})	0.65	0.76	1.18	0.23	0.34	1.52
Integrin beta-1 (Ser^{263})	0.42	0.57	0.82	2.23	2.27	1.02

Table 3. Fatty acid composition of RAT total lipid

Fatty acid		% of total fatty acids		
		Sham	**Ovx**	**Ovx+E2**
C12:0	Lauric acid	0.04 ± 0.01	0.05 ± 0.01*#	0.04 ± 0.01
C14:0	Myristic acid	0.62 ± 0.06	0.75 ± 0.07*#	0.67 ± 0.11
C16:0	Pamitic acid	18.7 ± 1.4	21.2 ± 1.4*	20.4 ± 1.2*
C18:0	Stearic acid	3.35 ± 0.21	3.21 ± 0.37	3.2 ± 0.15
C20:0	Arachidinic acid	0.06 ± 0.01	0.04 ± 0.01*	0.05 ± 0.01*
C22:0	Behenic acid	0.018 ± 0.001	0.009 ± 0.001*#	0.012 ± 0.001*
C16:0/C18:0		5.75 ± 0.39	6.67 ± 0.88*	6.3 ± 0.57
∑ SFA		22.8 ± 1.5	25.3 ± 1.5*#	24.4 ± 1.3
C14:1n-7	Myristoleic acid	0.02 ± 0.01	0.03 ± 0.01*#	0.02 ± 0.01
C16:1n-7	Palmitoleic acid	1.55 ± 0.3	2.36 ± 0.59*#	1.8 ± 0.52
C18:1n-9	Oleic acid	27.7 ± 1.2	27.5 ± 1.7	27.2 ± 0.9
C18:1n7	cis-vaccenic acid	2.32 ± 0.18	2.23 ± 0.12	2.31 ± 0.17
C20:1n9	Eicosenoic acid	0.18 ± 0.02	0.15 ± 0.01*	0.16 ± 0.01*
C18/C18:1		0.11 ± 0.01	0.11 ± 0.02	0.11 ± 0.01
C16:0/C16:1n-7		12.2 ± 1.7	9.38 ± 1.8*#	12.3 ± 2.9
∑ MUFA		31.8 ± 1.3	32.4 ± 2.3	31.4 ± 1.4
C18:3n-3	Alpha-linolenic acid	1.50 ± 0.18	1.81 ± 0.14*	1.84 ± 0.05*
C20:5n-3	Eicosapentaenoic acid (EPA)	0.02 ± 0.01	0.03 ± 0.001*	0.03 ± 0.01*
C22:5n-3	Docosapentaenoic acid (DPA)	0.09 ± 0.02	0.09 ± 0.02	0.09 ± 0.02
C22:6n-3	Docosahexaenoic acid (DHA)	0.16 ± 0.05	0.15 ± 0.06	0.15 ± 0.03
∑ n-3		1.75 ± 0.28	2.08 ± 0.17*	2.11 ± 0.08*
C18:2n-6	Linoleic acid	40.14 ± 2.0	37.1 ± 2.8*	38.5 ± 2.3
C18:3n-6	Gamma-linoleic acid	0.07 ± 0.02	0.1 ± 0.01*	0.09 ± 0.02*
C20:2n-6	Eicosadienoic acid (EDA)	0.19 ± 0.02	0.16 ± 0.03*	0.17 ± 0.2*
C20:3n-6	Dihomo-gamma linoleic acid	0.14 ± 0.02	0.14 ± 0.02	0.15 ± 0.01
C20:4n-6	Arachidonic acid (AA)	0.63 ± 0.17	0.69 ± 0.18	0.74 ± 0.14
C22:4n-6	Docosatetraenoic acid	0.23 ± 0.08	0.19 ± 0.06	0.20 ± 0.04
∑ n-6		41.4 ± 2.2	38.4 ± 3.0*#	39.9 ± 2.4
∑ n-6/ ∑ n-3		24.1 ± 3.9	18.5 ± 0.7*	18.9 ± 0.9*
∑ PUFA		43.1 ± 2.4	40.5 ± 3.2	42.1 ± 2.5
∑ SFA/ ∑ PUFA		0.53 ± 0.07	0.63 ± 0.08*	0.58 ± 0.06

Data presented as means ± SEM of the % of total FAs. n=6 for each group. SFA: saturated fatty acids; MUFA: monounsaturated fatty acids; PUFA: polyunsaturated fatty acids; t: trans fatty acids. *$p < 0.05$ *vs* Sham; #$p < 0.05$ Ovx *vs* Ovx+E2